Iris Recognition Through Edge Detection Methods: Application in Flight Simulator User Identification

Sundas Naqeeb Khan[1*], Samra Urooj Khan[2], Onyeka Josephine Nwobodo[3], Krzysztof Adam. Cyran[4]
Department of Graphics, Computer Vision and Digital Systems, Silesian University of Technology, Gliwice, Poland[1, 3, 4]
Faculty of Electrical and Electronic Engineering, Universiti Tun Hussien Onn Malaysia (UTHM), Johor, Malaysia[2]

***Abstract*—To meet the increasing security requirement of authorized users of flight simulators, personal identification is becoming more and more important. Iris recognition stands out as one of the most accurate biometric methods in use today. Iris recognition is done through different edge detection methods. Therefore, it is important to have an understanding of the different edge detection methods that are in use these days. Specifically, the biomedical research shows that irises are as different as fingerprints or the other patterns of the recognition. Furthermore, because the iris is a visible organism, its exterior look can be examined remotely using a machine vision system. The main part of this paper delves into concerns concerning the selection of the best results giving method of the recognition. In this paper, three edge detection methods, namely Canny, Sobel and Prewitt, are applied to the image of eye (iris) and their comparative analysis is discussed. These methods are applied using the Software MATLAB. The datasets used for this purpose are CASIA and MMU. The results indicate that the performance of Canny edge detection method is best as compared to Sobel and Prewitt. Image quality is a key requirement in image-based object recognition. This paper provides the quality evaluation of the images using different metrics like PSNR, SNR, MSE and SSIM. However, SSIM is considered best image quality metric as compared to PSNR, SNR and MSE.**

Keywords*—*Identification; authentication; detection; canny; Sobel; Prewitt; PSNR; SNR; SSIM; MSE

I. Introduction

In the paper, the automatic authorization of flight simulator users is considered. Large pilot training centers require an increased security level to minimise the probability of unauthorised usage of the devices. In addition, pilot training procedures have to be rigorously verified as the number of hours spent in the simulator during virtual flights serves as proof of sufficient practice level for the pilot (in addition to hours spent in actual aircraft). Therefore, flights on certified flight simulators can be (to some extent defined by Regulatory Authorities) used as an alternative and cheaper counterpart to actual training flights because current flight simulators mimic the cockpit of the aircraft and the environment outside of the aircraft with great fidelity for maintaining the expertise of both civilians and military aircrews.

Flight simulators have significantly impacted the expertise and cutting-edge use of training pilots and aircraft crews, resulting in increased efficiency as training will not be affected by things like bad weather, aircraft space restriction and aircraft availability. It allows pilots to experience a wide range of flight scenarios and conditions to experience real-life situational awareness. Haslbeck et al. [1] reported an experimental study where pilots with varying levels of experience and training had to fly 45 minutes of approach landing scenarios and compare their performance to manual flying. Their findings showed that a pilot with high levels of flight simulator training exhibits high and homogenous performance. Enhancing the pilot's monitoring techniques during the training session may aid in determining a pilot's performance in a flight simulator by employing object detection algorithms to analyze the pilot's head movement and eye gaze. The trainer can utilize this data to pinpoint areas where the pilot might benefit from extra instruction or development [2]. Škvareková et al. [3] research shows using eye tracking technologies to monitor eye movement to assist pilot training in flight simulators.

Its fidelity is not limited to training the pilot and aircrew. They are also used for research, enabling designers to examine the effects of various alternatives without spending money or waiting for various prototypes to be built [4], conduct aircraft incident investigations, and better understand ergonomic relationships [5]. Flight simulation is a multidisciplinary field that draws on many different areas of study, including human factors, motion actuation, sensory perception and visual image processing [6 - 7].

The use of flight simulators in pilot training has become indispensable, likewise the need to secure this gadget by minimising unauthorised users. They offer secure, affordable and adaptable alternatives to teach pilots in various scenarios and settings, enhancing their knowledge, self-assurance and decision-making capabilities [8 - 9]. As evident in Fig. 1, the flight simulator developed in the WrightBroS project is depicted.

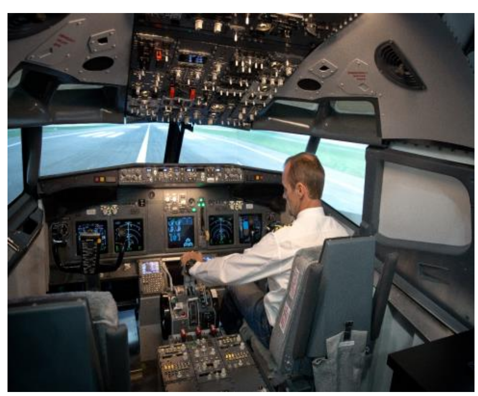

Fig. 1. MCC FNTP II flight simulator of boeing 737.

*Corresponding author

The technology of digital imaging helps to manipulate digital photos using computers. The pre-processing, enhancement and display extraction of information is three general phase's frameworks where all forms of data must pass while employing digital technologies. A digital image consists of a limited number of elements, each having a specific position and values. These items are known as picture elements, pixels and image elements. The term pixel is the most usable form of the digital picture elements [10 - 11].

The word iris is a classic term. As with the colored part of the external eye, iris appears as of the 16th century and was taken to denote the variegated look of its structure [12]. The human iris contains many characteristics including freckles, crown, strips, furshes, crypts, etc., and is the annular section between pupils and sclera. In contrast to other biometric characteristics based on personal authentication recognition of iris can achieve great precision because of the rich texture of iris patterns [13]. Fig. 2 shows the full eye image with all its features.

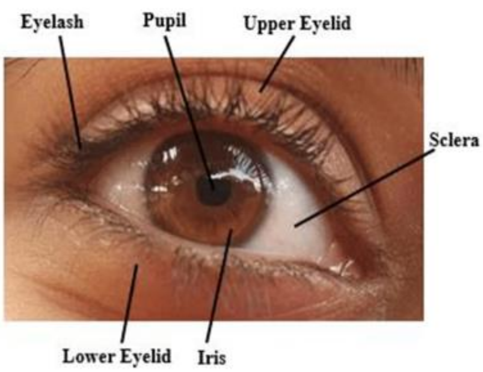

Fig. 2. A general view of a human eye [15].

Although the history of iris recognition comes back to the 19th century, automatic iris recognition is a newly emergent issue in biometrics [14]. It seems that the French ophthalmologist Alphonse Bertillon was the first one who proposed the use of iris pattern (color) as a basis for personal identification. Flom and Aran Safir suggested also using the iris as the basis for a biometric in 1981 [15].

Regarding the level of precision, it is apparent the fact that iris recognition requires an excellent recognition rate and, as a result, applying edge detection approaches for this problem are efficient, which has not been extensively investigated in previous studies for such systems.

The main goal of this study is to use different techniques to detect the edges of the images and then examine the results to see which technique effectively detects and sharpens the edges. For this study, the following primary objectives have been proposed:

- To recognize iris through edge detection methods.
- To compare the results of the selected edge detection methods.
- To check the performance of the methods via evaluation measures.

II. Literature Review

This section includes algorithms, methods, procedures, processes, approaches, techniques, detectors, models, and filters, as well as all of the history research where their links were used as evolutionary and provided the optimized form of solutions for edge detection issues. As a result of the researcher's efforts, the number of filters has grown over time. They worked hard to improve, enhance, co-relate, and collaborate on various methods to solve edge detection problems in image processing, and they created new, modified methods.

Edge detection is at the forefront of image processing for object detection, understanding edge detection methods are critical. ISEF, Canny, Marr-Hildreth, Sobel, Kirsch, Lapla1 and Lapla2 and Hough transform are the most important and widely used edge detection techniques [16].

Edge detection methods are further categorized into Gradient based (1st derivative order) and Gaussian based (2nd derivative order). Gradient based methods can be classified into Sobel, Prewitt, Robert, Kirsch, Robinson and Frei-Chen. Gaussian based methods are divided into Canny edge detection, Difference of Gaussian, Laplacian of Gaussian (like, Marr-Hildreth method) and Zero Crossing [17 – 18]. Fig. 3 shows the taxonomy of the methods which are related to the detection of the iris.

The Canny edge detector is a common and effective edge feature detector that is utilized in many computer vision algorithms as a pre-processing step [19 – 20]. The steps in the Canny Edge Detection Algorithm are as follows [21]:

Step 1: Apply a Gaussian filter to the image to smooth it out.
Step 2: Using finite-difference approximations for partial derivatives, compute the gradient magnitude and orientation.
Step 3: Apply non-maxima suppression to the gradient magnitude, then detect and link edges using the double thresholding approach.
Step 4: The operator that optimizes the product of signal-to-noise ratio and localization is approximated by the Canny edge detector. It is usually a Gaussian's first derivative.

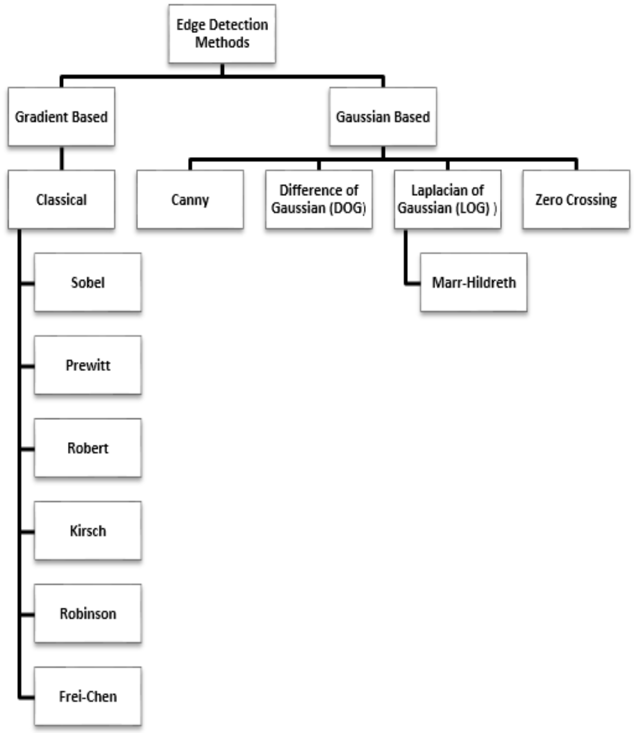

Fig. 3. Taxonomy of image detection methods.

For edge detection, the Sobel operator is utilized. The Sobel approach finds image edges using the derivative approximation in the edge function [22]. The Sobel algorithm is broken down into four steps [23]:

Step 1: Converting the image to grayscale is the first step.
Step 2: Using the Sobel-x filter to enlarge the grey image.
Step 3: Applying the Sobel-y filter to the grey image.
Step 4: Determining the magnitude and direction of the gradient.

In image processing, the Prewitt operator is commonly employed in edge detection techniques. It is a discrete differentiation operator that computes an approximation of the picture intensity function's gradient. The Prewitt operator returns either the relevant gradient vector or the norm of this vector at each location in the image [24]. The Prewitt method is broken down into four steps [17]:

Step 1: Read an image as input.
Step 2: Create a grayscale image from a true-color RGB image.
Step 3: Double-click the image to enlarge it.
Step 4: Fill the filtered image matrix with zeros before starting.

The literature collects data on iris-based identification methods. It also eloquently discusses each method's effectiveness and highlights areas for future investigation for concerned scholars. The results of this study may be utilized to enhance iris detection system development.

TABLE I. SUMMARY OF THE ARTICLES ALONG THEIR PROMINENT METHODS, DATASET AND RESULTS

Biometric Trait	Ref.	Methods	Dataset	Results
Iris	[25]	Circular Hough transform and convolutional neural network	CASIA-V3	Left and Right-side iris recognition accuracy is 99%.
	[26]	Hough transform and region-based convolutional neural network	CASIA	99.14% of accuracy
	[27]	Hough transform and region-based convolutional neural network	CASIA-V4	Accuracy is 96.3%
	[28]	Convolutional neural network	IITD	97.46% of accuracy
	[29]	Hough transform with canny edge detection	CASIA-VI	Accuracy is 93.33%
	[30]	Circular Hough transform with active contour	CAISA	88.3% of accuracy

Table I describes numerous iris recognition methods along dataset and their results which learned from earlier references. Some of these articles address the entire recognition procedure while others focus on the methodology only.

III. MATERIALS AND METHODS

The main step is pre-processing, feature extraction and matching where edge detection methods are used and try to improve the efficiency. The pre-processing steps comprise the conversion of the image from a color image to gray-scale image, iris localization, edge detection, filtration, etc. Now the Fig. 4 represents the proposed model for image processing especially iris recognition.

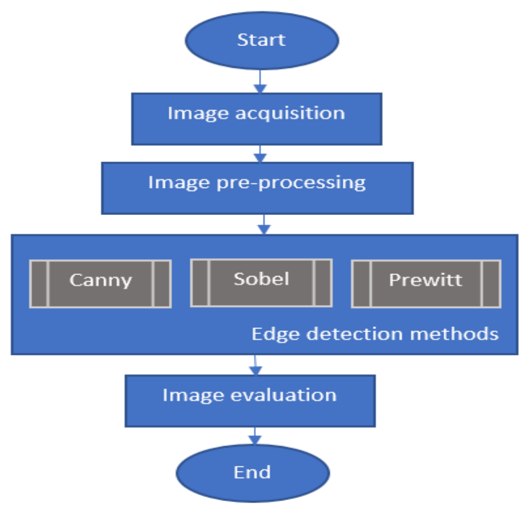

Fig. 4. Proposed model for iris recognition.

According to Fig. 5, this section covers the project's basic flow, the suggested iris recognition model, and the project flow chart in a more organized manner. Level 1, Level 2 and Level 3 of Project flow chart are demonstrated in detail. The activity of getting an image from a source is known as image acquisition; image segmentation is the process of separating an image into sections or regions; and feature extraction techniques are used to obtain features that will be useful in image classification and recognition. Edge detection will be done by using Canny, Sobel and Prewitt edge detection methods for iris recognition.

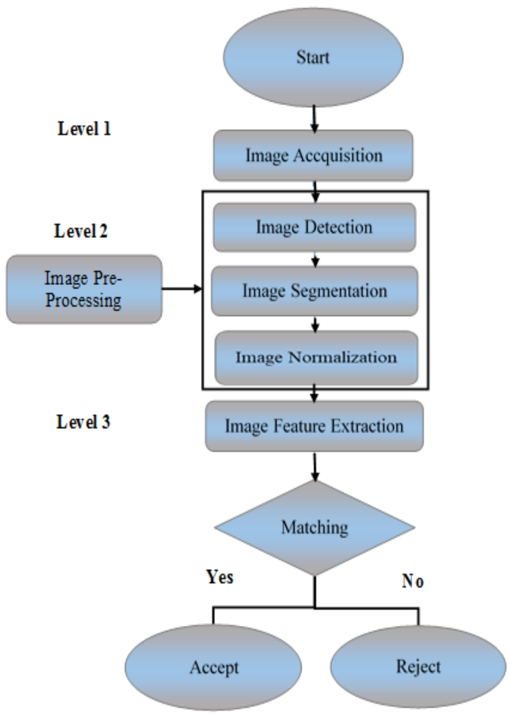

Fig. 5. Project flowchart.

IV. Results and Discussion

This experiment represents the analysis of the various methods of edge detection. Edge detection is a fundamental step, and it is necessary to point out the true edges to get the best results. That is why it is important to choose a good edge detection method. The experiment was done on MATLAB software and tested with the eye image. To extract the clean edges is main objective. In this experimental analysis, the results of the five images from the CASIA dataset are obtained in Table II. The results of the methods of Canny, Prewitt, and Sobel on the original images are analyzed. After this experimental analysis, it is found that the canny edge detection method is working well in comparison with Sobel and Prewitt. In the empirical testing, it can be seen clearly that Prewitt and Sobel do not produce good sharp edges. Sobel is not very accurate in edge detection as it detects thick and rough edges and does not give appropriate results. Analysis shows that canny extraction of image features without affecting and altering the feature is good. It is observed that the canny edge detector method is a better edge detector method of forming the edges for inner as well as outer lines. Hence, it is experimentally proved that canny is the most efficient and optimal method of edge detection.

Here, Table III illustrates the results of five images from the MMU dataset used in this experiment. After experimental examination, it is clear that canny method is more accurate rather than the Prewitt and Sobel. These are simple in evaluation separately then it improves the image results in the form of features extraction.

A. Image Quality Metrics for CASIA Dataset

For five images of CASIA Dataset, PSNR (Peak Signal to Noise Ratio), SNR (Signal to Noise Ratio), MSE (Mean Square Error), SSIM (Structure Similarity Index Method) for different methods have been calculated. Noisy images are converted into filtered images by using Gaussian noise to the images and filtered by Gaussian Filter and then results for all metrics are compared. From Table IV, it can be seen that all metrics have given almost consistent results. But SSIM is normalized as compared to PSNR, SNR and MSE. So, from this analysis the SSIM is comparatively better than MSE, SNR and PNSR metrics from human visual perspective.

B. Image Quality Metrics for MMU Dataset

Similarly, in Table V now, it is calculated PSNR, SNR, MSE, and SSIM for five images from the MMU Dataset. However, SSIM is balanced in terms of visibility, whereas MSE and PSNR are not. As a result, SSIM can be dealt in a more straightforward manner than MSE and PSNR. This is because MSE and PSNR are absolute errors, whereas SSIM produces perception and image errors. When the noise level rises, the recovery quality of the output image worsens as well. So, SSIM is better amongst all other metrics.

C. Comparative Analysis of the CASIA and MMU Dataset with Different Approaches

In Table VI, there are a number of articles presents their empirical testing results in the form of accuracy for iris recognition. Besides this, the evaluation datasets are also described for the further processing of the testing whereas the 99.7% ratio of the accuracy according to the CASIA-V1.0 and this gives the results from [38]. The result of 97.2% accuracy of the CASIA-V3.0/V4.0 is presented in the good form of the [38]. In [37], MMU-V1.0 dataset of the iris provides the high form of the ratio which is 99.45% accuracy as compare to the other research articles.

TABLE II. EDGE DETECTION METHODS APPLIED ON CASIA DATASET

Image No.	Original	Canny	Prewitt	Sobel
1				
2	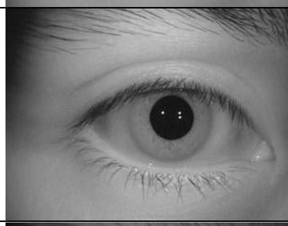			
3	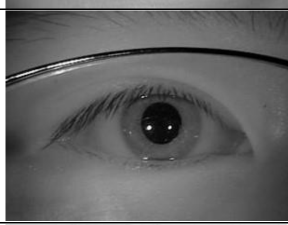		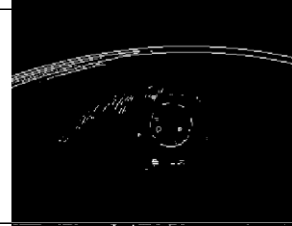	
4		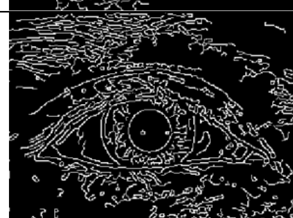	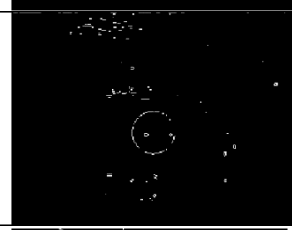	
5			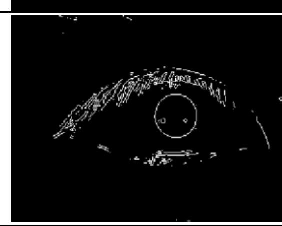	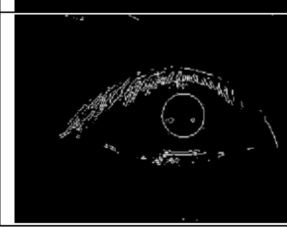

TABLE III. EDGE DETECTION METHODS APPLIED ON MMU DATASET

Image No.	Original	Canny	Prewitt	Sobel
1	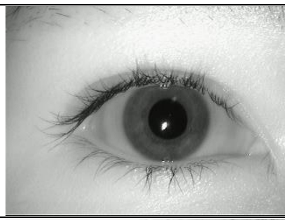		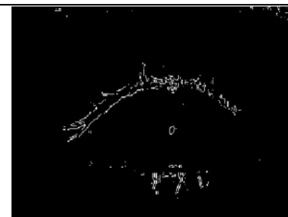	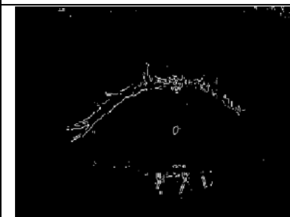
2		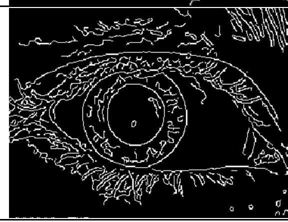		
3	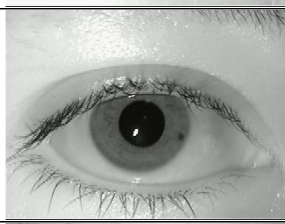		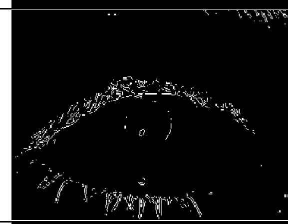	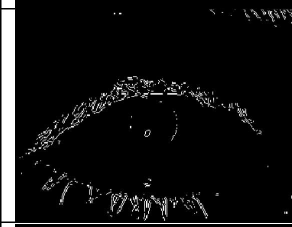
4		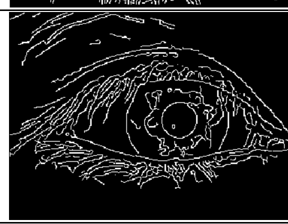	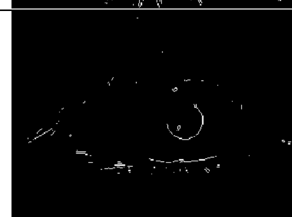	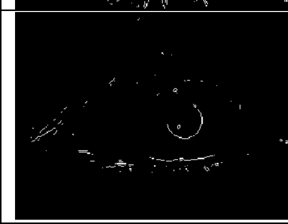
5	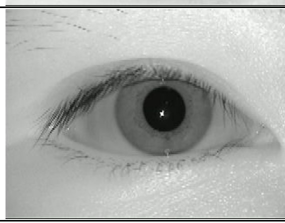	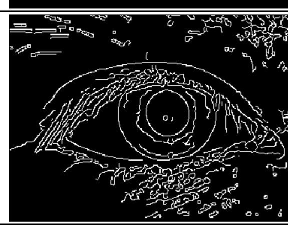	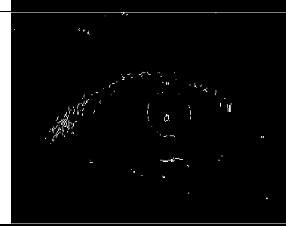	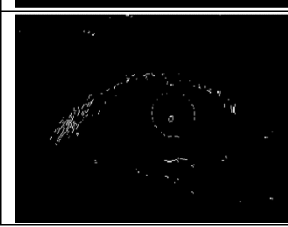

TABLE IV. IMAGE QUALITY METRICS FOR CASIA DATASET

Image No.	Noisy Image (Gaussian Filter 0.09)	Filtered Image	PSNR	SNR	MSE	SSIM
1			17.4355	10.8874	1179.1391	0.146182
2			17.4461	11.5067	1170.7628	0.187546
3			17.4486	9.2077	1170.0936	0.169675
4			17.4835	9.0891	1160.7283	0.209050
5		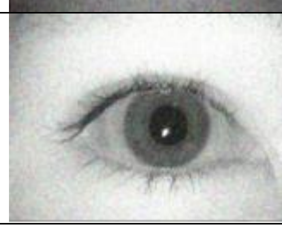	18.5162	15.7319	915.0796	0.280726

TABLE V. IMAGE QUALITY METRICS FOR MMU DATASET

Image No.	**Noisy Image (Gaussian Filter 0.09)**	**Filtered Image**	**PSNR**	**SNR**	**MSE**	**SSIM**
1			18.5219	15.7376	913.8797	0.280778
2		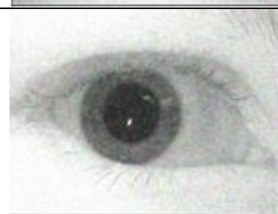	18.7602	16.0665	865.0809	0.268316
3	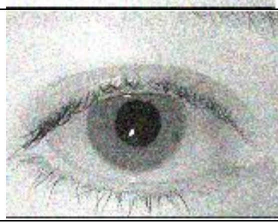	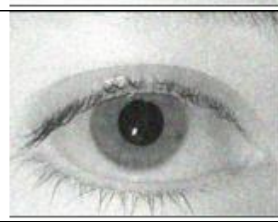	18.0561	14.7173	1017.3440	0.299774
4			18.0612	14.8339	1016.1554	0.239681
5	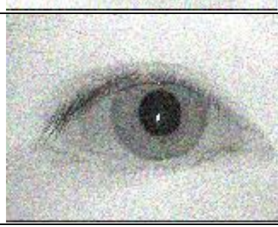	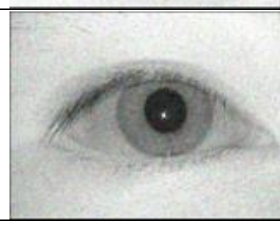	18.0562	14.9164	1017.3274	0.244308

TABLE VI. COMPARATIVE ANALYSIS OF THE DIFFERENT APPROACHES ALONG ACCURACY FOR EVALUATION

Ref.	Methods	Evaluation	Accuracy
[31]	Hough transform	CASIA-V3.0/V4.0	93.12%
[32]	Fourier transform	CASIA-V1.0	96%
[33]	Neural network	CASIA-V3.0/V4.0	95.36%
[34]	Principle component analysis	CASIA-V3.0/V4.0	90%
[35]	Refine connect extend smooth	CASIA-V3.0/V4.0	95.1%
[35]	Refine connect extend smooth	CASIA-V1.0	96.48%
[38]	Leading edge detector	CASIA-V1.0	99.7%
[38]	Leading edge detector	CASIA-V3.0/V4.0	97.2%
[36]	Hough transform along hamming distance	MMU-V1.0	95.66%
[37]	Edge detection operators	MMU-V1.0	99.45%
[38]	Leading edge detector	MMU-V1.0	98%
[39]	Morphological operators	MMU-V1.0	98.78%

D. Graphical Analysis of Image Quality Metrics for CASIA Dataset

Fig. 6 illustrates the PSNR for the CASIA dataset is almost constant, i.e., 17.4, from starting image CI-1 (CASIA Image) to image CI-4. After CI-4, there is a sharp increase in the PSNR. In C-5, there is a gradually change in values from 17.4 to 18.5 which shows an abrupt change as compared to four other images. CI-5 image shows PSNR value 18.5162 which is high as compared to other values. High value of PSNR gives better resolution of image. Therefore, CI-5 gives better result in this case.

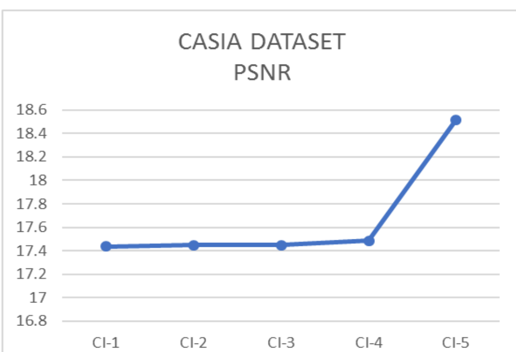

Fig. 6. PSNR of CASIA dataset.

The fluctuation shows in Fig. 7 with the value of SNR between first and forth image while there is a hike between fourth and fifth image. CI-1 image shows SNR value 10.8, then there is a slight change and CI-2 image shows SNR value 11.5. Image CI-3 shows abrupt change with SNR value 9.2. CI-4 image with minor change shows SNR value 9.0. CI-5 image shows SNR value 15.7. In this graph image CI-5 shows good resolution because of high value.

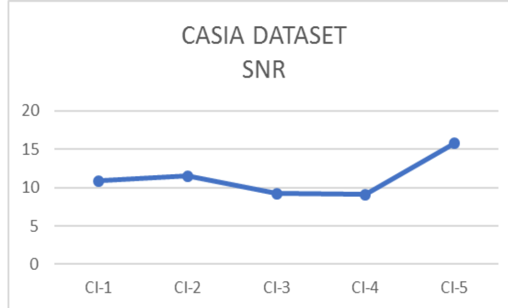

Fig. 7. SNR of CASIA dataset.

According to the Fig. 8, the SSIM value for each preceding image is larger than the previous one except for the image CI-3. SSIM values ranges from -1 to 1. -1 is the lowest value which shows that there is no similarity between images and 1 value is considered to be the highest value which shows that there is a high similarity between images. Now here, CI-1 image provides better resolution than all other images with SSIM values.

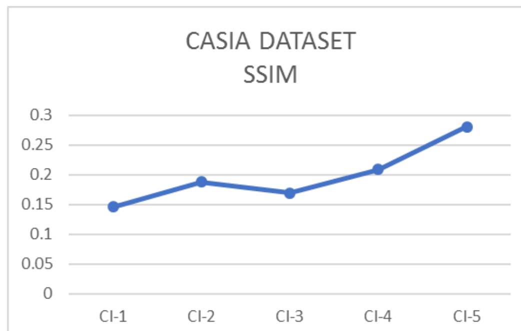

Fig. 8. SSIM of CASIA dataset.

Fig. 9 presents that the value of MSE for the sequentially four images are almost constant while for the 5th image, there is a drop in the value of MSE. The MSE value is the average difference between all pixels in the image. A greater discrepancy between the original and processed image is indicated by a higher MSE value. MSE value is positive. A value close to 0 is considered a better value. So, image 4 with MSE value 1160.7283 shows better result in CASIA dataset

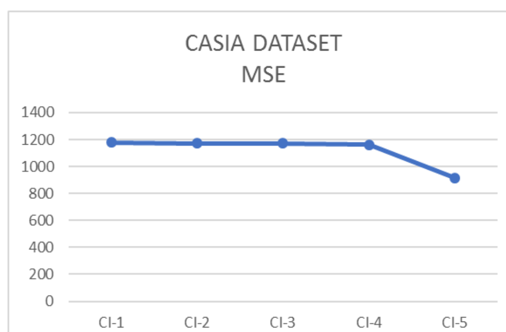

Fig. 9. MSE of CASIA dataset.

E. Graphical Analysis of Image Quality Metrics for MMU Dataset

The PSNR block calculates the PSNR between two images in decibels. This ratio is used to compare the features of the original images and filtered Image. PSNR reflects the peak error measurement. MMUI-1 shows PSNR value 18.5219 while MMUI-2 shows PSNR value 18.7602. MMUI-3, MMUI-4 and MMUI-5 represent less constant PSNR values as compared to MMUI-1 and MMUI-2 which shows MMUI-2 with greater PSNR value (18.7602) is better result in Fig. 10.

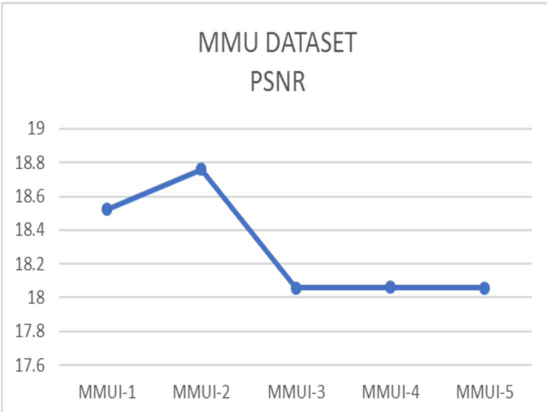

Fig. 10. PSNR of MMU dataset.

Therefore, Fig. 11 represents results of SNR values for MMU Dataset. The SNR measures how well a desired signal compares to background noise. MMUI-1 shows better result in graph as compared to MMUI-3, MMUI-4 and MMUI-5. As there is a decline after MMUI-2, so MMUI-1 is finer among all values.

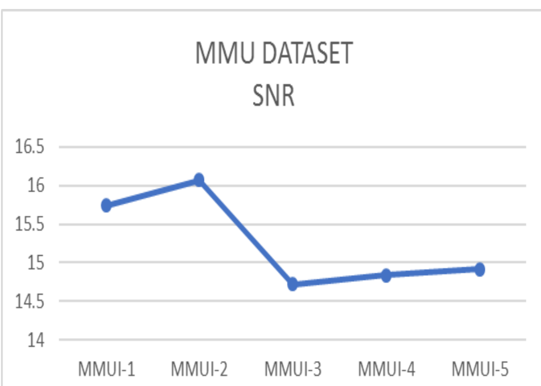

Fig. 11. SNR of MMU dataset.

The results of SSIM values for MMU Dataset are illustrated in Fig. 12. MMUI-1 shows 0.280778 SSIM result as there is a fall off after image 1. MMUI-2 shows 0.268316 SSIM value in the meanwhile there is a lift after image 2. MMUI-3 present 0.299774 SSIM value while there is a turn down in MMUI-4 and MMUI-5. So, MMUI-3 provides better result.

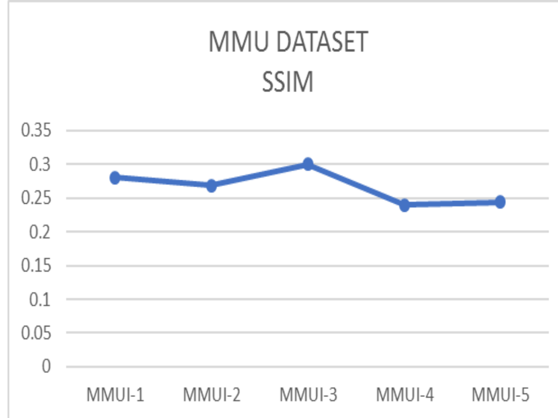

Fig. 12. SSIM of MMU dataset.

In Fig. 13, MSE value for MMUI-1 lies between 900 and 950. There is sudden fall after image 1; MMUI-2 shows MSE values between 850 and 900. After image 2, there is abrupt change in graph. MMUI-3, MMUI-4 and MMUI-5 show constant values at their peak level values between 1000 and 1050. A value close to 0 is considered a better value. So, MMUI-2 with exact MSE value 865.0809 shows better result in MMU dataset as it is the lowest value as compared to all other values in the graph.

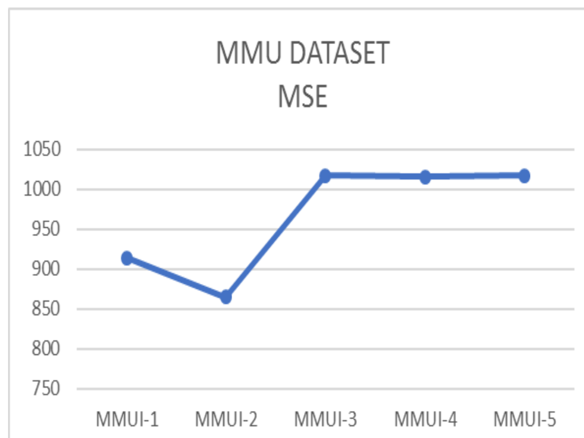

Fig. 13. MSE of MMU dataset.

F. Comparative Analysis of Image Quality Metrics

The Fig. 14 demonstrates the comparative analysis for the PNSR values of CASIA and MMU dataset. A major difference can be seen between two datasets. The CASIA dataset shows constant result for four images and then there is an increase in the graph for image 5. The MMU dataset shift for three images and then shows constant result for 4 and 5 images. First four images of MMU dataset are strongly preferred as compared to first four images of CASIA dataset because of high PNSR value. But in comparison, 5th image of CASIA dataset is better than 5th image of MMU dataset. So, in this graph MMU dataset results are good in the form of PSNR.

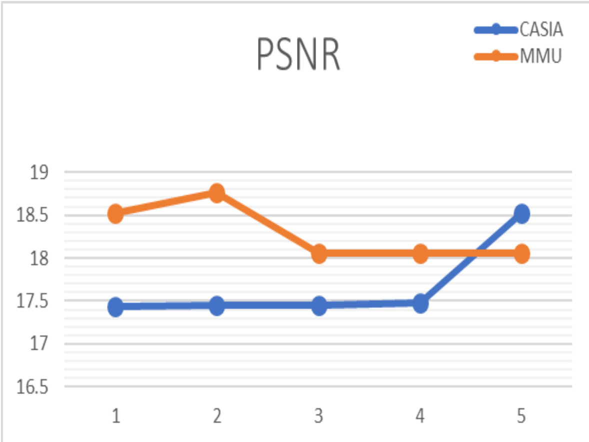

Fig. 14. Comparative analysis of PSNR.

In the Fig. 15 graphical analyses, SNR values of CASIA and MMU dataset are compared. Differences between two datasets distinguish both of them. The CASIA dataset shows oscillation for five images in the graph. On the other side, MMU dataset describes shift for three images and then shows constant result for 4 and 5 images. First four images of MMU dataset are strongly preferred as compared to first four images of CASIA dataset because of high SNR value. But in comparison, 5th image of CASIA dataset is better than 5th image of MMU dataset because of slight high difference. So, in this graph MMU dataset results are better according to the SNR.

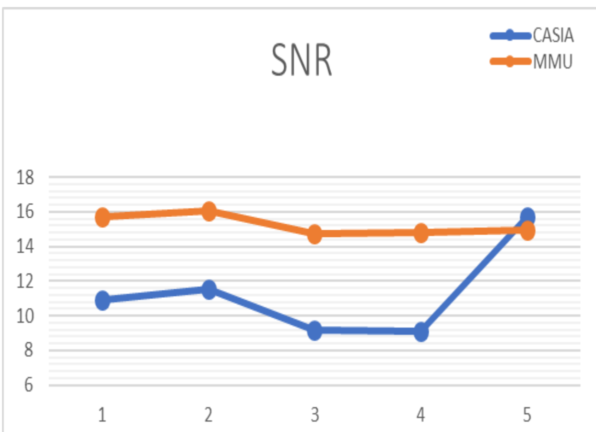

Fig. 15. Comparative analysis of SNR.

The SSIM values of CASIA and MMU dataset are analyzed in Fig. 16. Up and downs between two datasets distinguish rather first four images of MMU dataset are better as compared to first four images of CASIA dataset because of high values near to zero. But in comparison, 5th image of CASIA dataset is better than 5th image of MMU dataset as slightly high difference. So, MMU dataset results are strongly preferred.

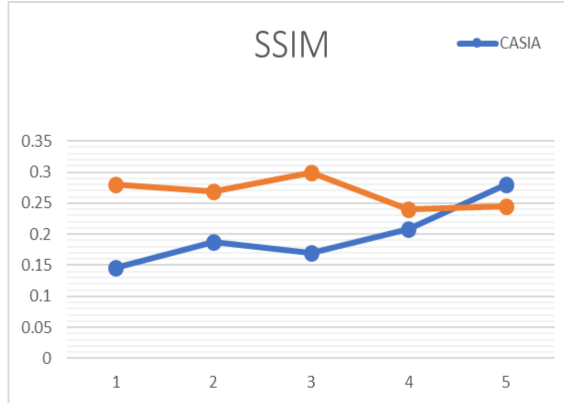

Fig. 16. Comparative analysis of SSIM.

The graphical analysis shows MSE values of CASIA and MMU dataset in Fig. 17. The CASIA dataset shows variation for five images in the graph. Besides this, MMU datset represents rise and fall for 5 images. First four images of MMU dataset are better as compared to CASIA dataset because of low values near to zero. But in comparison, 5th image of CASIA dataset is better than 5th image of MMU dataset because of lowest value. So, in this graph MMU dataset results are strongly good.

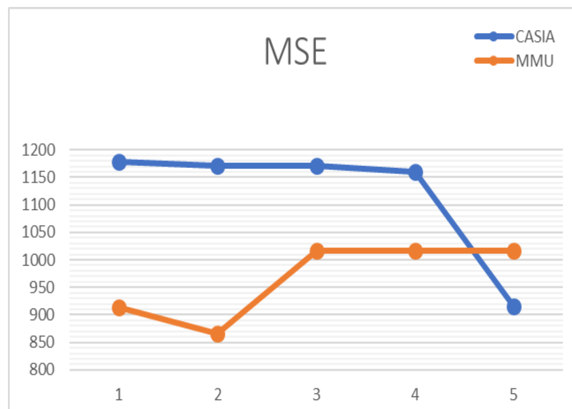

Fig. 17. Comparative analysis of MSE.

V. Conclusion

This research covers all of the conclusions from the research methods. The main objectives are completed by comparative analysis of the edge detection methods which is the required tasks. Three edge detection methods have been proposed for identifying the borders of objects within images from two benchmark datasets (CASIA, MMU), removing blurriness from the findings through edge detection techniques, and evaluating performance using parameters. The study's accomplishments are revealing a considerable improvement in image quality and crispness. This study also includes suggestions for future improvements that other researchers should explore in order to concentrate on the experimental results, obtained the defects detected in this work, and apply the highlighted work to other areas that need attention.

In the future, a new filtered method can be created to overcome the constraint in order to improve image quality and enrich the image by minimizing noise.

ACKNOWLEDGMENT

The authors would like to acknowledge that this paper is based on the results achieved within the WrightBroS project. This project has received funding from the European Union's Horizon 2020 research and innovation program under the Marie Skłodowska-Curie grant agreement No 822483. Supplementarily, this research work has been co-financed from Polish financial resources for science in 2019-2023 and conferred for the implementation of the co-financed international project.

Disclaimer. The paper reflects only the author's view, and the Research Executive Agency (REA) is not responsible for any use that may be made of the information it contains.

CONFLICT OF INTEREST

The authors confirm that there is no conflict of interest involve with any parties in this research study.

REFERENCES

[1] Haslbeck, A. et al. (2014) 'A flight simulator study to evaluate manual flying skills of airline pilots', in Proceedings of the Human Factors and Ergonomics Society. Human factors an Ergonomics scociety Inc., pp. 11-15. Available at: http://doi.org/10.1177/1541931214581003.

[2] Lefrançois, O., Matton, N. and Causse, M. (2021) 'Improving airline pilots' visual scanning and manual flight performance through training on skilled eye gaze strategies', Safety, 7(4). Available at: https://doi.org/10.3390/safety7040070.

[3] Skvarekova, I. et al. (2020) 'Eye Track Technology in Process of Pilot Training Optimization', in NTinAD 2020 - New Trends in Aviation Development 2020 - 15th International Scientific Conference, Proceedings. Institute of Electrical and Electronics Engineers Inc., pp. 206–210. Available at: https://doi.org/10.1109/NTAD51447.2020.9379071.

[4] Smaili et al. (2017) CUSTOMER: European Commission Practices to identify and prevent adverse aircraft-and-rotorcraft-pilot couplings-A ground simulator perspective NLR-Netherlands Aerospace Centre. Available at: www.nlr.nl.

[5] Boril, J. et al. (2015) 'Aviation simulation training in the Czech air force', in AIAA/IEEE Digital Avionics Systems Conference - Proceedings. Institute of Electrical and Electronics Engineers Inc., pp. 9A21-9A213. Available at: https://doi.org/10.1109/DASC.2015.7311484.

[6] Boril, J., Jirgl, M. and Jalovecky, R. (2016) Use of Flight Simulators in Analyzing Pilot Behavior.

[7] Stroosma, O., Van Paassen, R. and Mulder, M. (2003) USING THE SIMONA RESEARCH SIMULATOR FOR HUMAN-MACHINE INTERACTION RESEARCH.

[8] Socha, V. et al. (2016) Training of Pilots Using Flight Simulator and its Impact on Piloting Precision

[9] Lazic, D.A., Grujic, V. and Tanaskovic, M. (2022) 'The role of flight simulation in flight training of pilots for crisis management', South Florida Journal of Development, 3(3), pp. 3624–3636. Available at: https://doi.org/10.46932/sfjdv3n3-046.

[10] Bauer, M.W., Knill, C. (2007): Management reforms in international organizations. – Nomos Verlagsgesellschaft 226p.

[11] Bauer, T.N., Bodner, T., Erdogan, B., Truxillo, D.M., Tucker, J.S. (2007): Newcomer adjustment during organizational socialization: a meta-analytic review of antecedents, outcomes, and methods. – Journal of Applied Psychology 92(3): 707-721.

[12] Berger, B.A. (2000): Incivility. – American Journal of Pharmaceutical Education 64(4): 445-450.

[13] Billsberry, J., Talbot, D., Hollyoak, B. (2011): The Social Construction of PE Fit. – In Academy of Management Journal-AMJ. Retrieved from: https://pureportal.coventry.ac.uk/en/publications/the-social-construction-of-pe-fit

[14] Brown, D., Warschauer, M. (2006): From the university to the elementary classroom: Students' experiences in learning to integrate technology in instruction. – Journal of Technology and Teacher Education 14(3): 599-621.

[15] Cole, M.S., Shipp, A.J., Taylor, S.G. (2016): Viewing the interpersonal mistreatment literature through a temporal lens. – Organizational Psychology Review 6(3): 273-302.

[16] Cortina, L.M., Kabat-Farr, D., Leskinen, E.A., Huerta, M., Magley, V.J. (2013): Selective incivility as modern discrimination in organizations: Evidence and impact. – Journal of Management 39(6): 1579-1605.

[17] Cortina, L.M., Magley, V.J., Williams, J.H., Langhout, R.D. (2001): Incivility in the workplace: incidence and impact. – Journal of Occupational Health Psychology 6(1): 64-80.

[18] George, J.M., Jones, G.R. (2001): Towards a process model of individual change in organizations. – Human Relations 54(4): 419-444.

[19] Giumetti, G.W., Hatfield, A.L., Scisco, J.L., Schroeder, A.N., Muth, E.R., Kowalski, R.M. (2013): What a rude e-mail! Examining the differential effects of incivility versus support on mood, energy, engagement, and performance in an online context. – Journal of Occupational Health Psychology 18(3): 297-309.

[20] Goparaju, L., Jha, C.S. (2010): Spatial dynamics of species diversity in fragmented plant communities of a Vindhyan dry tropical forest in India. – Tropical Ecology51 1: 55-65.

[21] Griffin, M.J., Abergel, A., Abreu, A., Ade, P.A., André, P., Augueres, J.L., Babbedge, T., Bae, Y., Baillie, T., Baluteau, J.P., Barlow, M.J. (2010): The Herschel-SPIRE instrument and its in-flight performance. – Astronomy & Astrophysics 518: 7p.

[22] Griffin, M.A., Neal, A., Parker, S.K. (2007): A new model of work role performance: Positive behavior in uncertain and interdependent contexts. – Academy of Management Journal 50(2): 327-347.

[23] Gruman, J. A., Saks, A.M., Zweig, D.I. (2006): Organizational socialization tactics and newcomer proactive behaviors: An integrative study. – Journal of Vocational Behavior 69(1): 90-104.

[24] Hershcovis, M.S., Barling, J. (2010): Towards a multi-foci approach to workplace aggression: A meta-analytic review of outcomes from different perpetrators. – Journal of Organizational Behavior 31(1): 24-44.

[25] Therar, H. M., Mohammed, L. D. E. A., & Ali, A. J. (2021, June). Multibiometric system for iris recognition based convolutional neural network and transfer learning. In IOP Conference Series: Materials Science and Engineering (Vol. 1105, No. 1, p. 012032). IOP Publishing.

[26] Jayanthi, J., Lydia, E. L., Krishnaraj, N., Jayasankar, T., Babu, R. L., & Suji, R. A. (2021). An effective deep learning features based integrated framework for iris detection and recognition. Journal of ambient intelligence and humanized computing, 12, 3271-3281.

[27] Azam, M. S., & Rana, H. K. (2020). Iris recognition using convolutional neural network. International Journal of Computer Applications, 175(12), 24-28.

[28] Alnahari, W. (2021). Convolutional Neural Network for Iris Recognition.

[29] Farouk, R. H., Mohsen, H., & Abd El-Latif, Y. M. (2022, March). Iris Recognition System Techniques: A Literature Survey and Comparative Study. In 2022 5th International Conference on Computing and Informatics (ICCI) (pp. 194-199). IEEE.

[30] Akinfende, A. S., Imoize, A. L., & Ajose, O. S. (2020). Investigation of iris segmentation techniques using active contours for non-cooperative iris recognition. Indonesian Journal of Electrical Engineering and Computer Science, 19(3), 1275-1286.

[31] Umer, S., Dhara, B. C., & Chanda, B. (2018). An iris recognition system based on analysis of textural edgeness descriptors. IETE Technical Review, 35(2), 145-156.

[32] Hamd, M. H., & Ahmed, S. K. (2018). Biometric system design for iris recognition using intelligent algorithms. International Journal of Modern Education and Computer Science, 12(3), 9.

[33] Ahmadi, N., & Akbarizadeh, G. (2018). Hybrid robust iris recognition approach using iris image pre-processing, two-dimensional gabor features and multi-layer perceptron neural network/PSO. Iet Biometrics, 7(2), 153-162.

[34] Abdulmunem, E., & Abbas, S. H. (2018). Iris recognition using SVM and BP algorithms. International Journal of Engineering Research and Advanced Technology (IJERAT), 4(5), 30-37.

[35] Ak, T. A., & Steluta, A. (2021). An iris recognition system using a new method of iris localization. International Journal of Open Information Technologies, 9(7), 67-76.

[36] Masek, L. (2003). Recognition of human iris patterns for biometric identification.

[37] Yuan, W., Lin, Z., & Xu, L. (2006, January). A rapid iris location method based on the structure of human eyes. In 2005 IEEE Engineering in Medicine and Biology 27th Annual Conference (pp. 3020-3023). IEEE.

[38] Ali, S. A., & George, L. E. (2013). New Approach of Iris Localization for Personal Identification. In International Conference on Information Technology in Signal and Image Processing (ITSIP-2013), Elsevier.

[39] Hashim, A. T., & Saleh, Z. A. (2019). Fast Iris localization based on image algebra and morphological operations. journal of university of Babylon for pure and Applied Sciences, 27(2), 143-154.